Journal of Thermal Analysis and Calorimetry, Vol. 57 (1999) 343-359

DETERMINATION OF THE RIGOROUS TRANSFER FUNCTION OF AN ISOTHERMAL TITRATION MICROCALORIMETER WITH PELTIER COMPENSATION

A. Velázquez-Campoy[1*], *O. López-Mayorga*[2] *and M. A. Cabrerizo-Vílchez*[1]

[1]Departamento de Física Aplicada, Facultad de Ciencias, Universidad de Granada E-18071 Granada
[2]Instituto de Biotechnología de la Universidad de Granada E-18071 Granada, Spain

Abstract

An old problem in Isothermal Titration Calorimetry is the accurate characterisation of the instrument, i.e. the determination of the instrumental transfer function. Normally, this calibration is performed electrically or through well known chemical reactions, but the transfer function parameters obtained by both methods generally do not agree: the first method normally yields smaller time constants than the second one. This fact is explained by the different path the heat flux takes towards the thermal sink. However, the time constants must be independent of the experiment type (electrical or chemical). In order to attain this independency, a realistic physical model of the system is developed taking into account the different heat sources and the paths in the system and using physically attainable (experimental and theoretical) inputs for testing the model. Important results from the model study are that the instrument is represented by different transfer functions, depending on the heat source location, and that the time constants are the same, regardless of the heat source location. A very simple and fast method based on such non-phenomenological physical model for obtaining the transfer function of an Isothermal Titration Microcalorimeter is applied here.

Keywords: control system, isothermal titration microcalorimetry, system theory

Introduction

Thermokinetic studies using isothermal microcalorimetry require an exhaustive dynamic characterisation of the calorimeter. The behaviour of a microcalorimeter is described by its transfer function. Therefore, the dynamic characterisation consists of a reliable determination of this function.

To date several methods have been proposed to solve this problem and they are classified into two general categories: transient response analysis [1–3] and frequency analysis [4–8].

These approaches present some problems: the impulse input is physically unattainable; the choice of the mathematical model has a big influence on the results;

* Author for correspondence: fax: +34 58 243214; e-mail: adrianv@goliat.ugr.es

1418–2874/99/ $ 5.00
© 1999 Akadémiai Kiadó, Budapest
Akadémiai Kiadó, Budapest
Kluwer Academic Publishers, Dordrecht

working with a sampled signal in the frequency domain poses some data processing problems; and the use of periodic signals is time consuming.

Therefore, a fast and precise method for obtaining the transfer function in the time domain has been designed. The development of a realistic physical model of the calorimeter is the key to the problem.

In all analysis procedures of real systems a mathematical representation of the physical model is required to study their features. Such model provides in idealised and simplified representation of the real system. The modelling of a system consists of three steps:

1. Selection of the elements that are relevant to the system behaviour.
2. Simplification of these elements.
3. Deduction of the system transfer function, based on fundamental physical laws applied to each element.

In practice, an exact mathematical representation of a complex system is impossible. However, formulating correct hypothesis about some system properties, can lead to an approximate but realistic model of the system. Comparison between the real and theoretical behaviour shows how far is the model a realistic representation of the real system.

In the model developed here the microcalorimetric unit of the isothermal titration microcalorimeter is represented by a lumped parameter model with three elements: sample, cell-temperature sensor ensemble and heat sink (Fig. 1). Each element has well defined thermal properties such as its heat capacity and heat transfer coefficient which are considered to be time invariant. These three elements have mutual interaction which is reflected in the differential equation set representing the individual energetic balances. These equations will be solved using the Laplace Transform method:

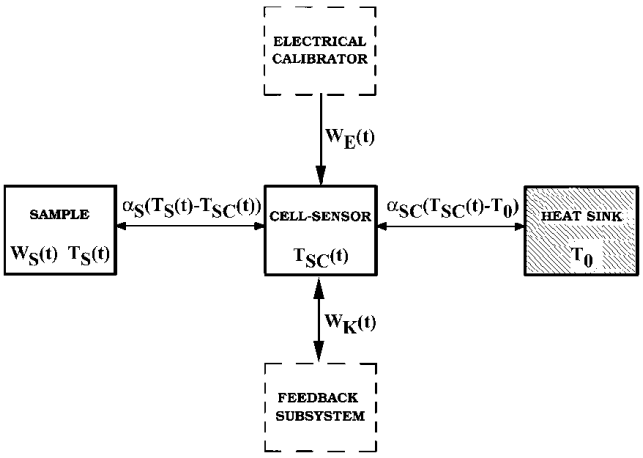

Fig. 1 Lumped-parameter model of the microcalorimetric unit with three elements: sample, cell-sensor and heat sink. α_S, α_{SC}: heat transfer coefficient between sample and cell-sensor set and cell-sensor set and heat sink. W_S, W_E, W_K: thermal power produced in the sample, by the electrical calibrator and by the feedback transducer. T_S, T_{SC}, T_0: sample, cell-sensor set and heat sink temperature

$$F(s) = L[f(t)] = \int_0^{+\infty} e^{-st} f(t)\mathrm{d}t \leftrightarrow f(t) = L^{-1}[F(s)] \quad (1)$$

where L is the Transform Laplace operator and s is the complex variable in the Laplace's transformed domain.

A very important aspect determining the behaviour of the instrument is the existence of different heat sources and, therefore, different heat flux paths in the microcalorimeter [9, 10]. The thermal effect source can be located in the sample itself (chemical reaction, viscous effect, ...), in the electrical heater on the cell-sensor set (electrical calibration) or in the compensator of the feedback control. We use the terms $W_S(t)$, $W_E(t)$ and $W_K(t)$ to indicate the heat flux from the corresponding source locations. An incorrect identification of the source would lead, as will be seen later, to a bad assignation of the poles and zeros (time constants) of the transfer function and, consequently, a wrong representation of the system.

Experimental

At present there are various types of isothermal titration microcalorimeters (ITM) available [11–13], but few have a high enough sensitivity for protein adsorption studies and, moreover, are very expensive. For that reason an ITM with digital control, based on the twin principle [14], has been designed and built in our laboratory for such studies.

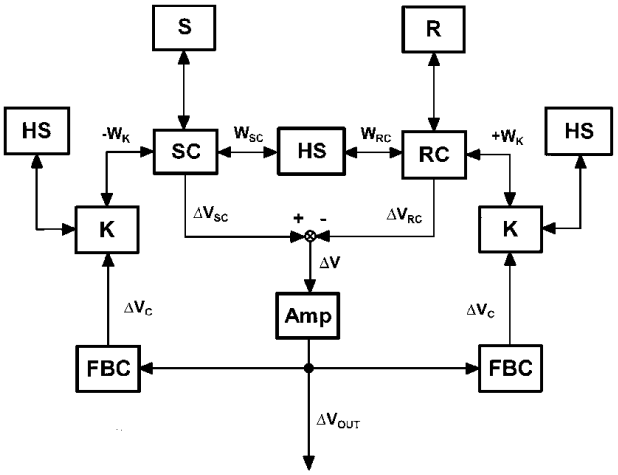

Fig. 2 Block diagram of the microcalorimetric system displaying the heat transfer processes and the signal generation. S, R: sample and reference SC, RC: sample and reference cell-sensor set. Amp, FBC, K: amplifier, feedback controller, feedback transducer (compensation thermopiles) and heat sink. W_{SC}, W_{RC}, W_K: thermal power transferred from the cell-sensor set to the heat sink in the sample and reference cells and thermal power generated by the feedback transducer on each cells. ΔV_{SC}, ΔV_{RC}, ΔV: voltage signals generated by the sensors in both cells and their difference. ΔV_{OUT}, ΔV_C: measured and feedback (compensated) voltage signal

Both gold cells, sample and reference, are filled with 5 ml of pure water for the calibration operations below described. In each cell a set of 66-junctions semiconductor (Bi_2Te_3) thermopiles is used as heat flux sensors (Seebeck effect). They are arranged electrically in serie and thermally in parallel, inserted between the outer cell wall and the thermal sink. The voltage difference between the flux sensor of the sample and reference cell is amplified (gain ca. 100000, in two stages) (INA 103 Burr-Brown) and then digitalized by means of a 16-bits A/D converter (DT2805/5716A Data Translation).

In our case there is a compensation control system which modifies the transfer function of the instrument [15, 16]. Compensation is achieved through a digital control system located in the feedback trajectory consisting of a computer and a 12-bits D/A converted (DT2805/5176A). The feedback signal is fed into an independent set of thermopiles in each cell. They generate a heat flux (Peltier effect) which attempts to restore thermal equilibrium (baseline). Feedback is produced in a bilateral way (Fig. 2). This presents some advantages with regard to the unilateral control, although both are formally identical. Bilateral feedback yields greater symmetry to the system leading to lesser thermal imbalance between sample and reference cell; as well as minimisation the unilateral Joule heat production by the feedback actuators and equality of the calibration constants for both exothermic and endothermic effect. The heat transfer processes and the signals generation that take place in the microcalorimeter are shown in the block diagram, Fig. 2.

Electrical calibrations were carried out passing a well defined electrical current through a resistor (161.94 Ω) made of 'molecular wire' wound around the sample cell wall. A Keithley 220 Programmable Current Source was used for this purpose.

Microcalorimeter model

Microcalorimeter transfer function for an open-loop control

Considering only the sample cell (SC), let us assume that there is a single thermal effect coming from the sample, $W(t)=W_S(t)$. The power balance leads to the differential equation set:

$$C_S \frac{dT_S(t)}{dt} = W(t) - \alpha_S(T_S(t) - T_{SC}(t))$$

$$C_{SC} \frac{dT_{SC}(t)}{dt} = \alpha_S(T_S(t) - T_{SC}(t)) - \alpha_{SC}(T_{SC}(t) - T_0) \quad (2)$$

where $T_S(t)$, $T_{SC}(t)$ and T_0 are the temperatures of the sample, cell-sensor set and heat sink; α_S and α_{SC} are the heat transfer coefficients between sample and cell-sensor set and between the cell-sensor set and the heat-sink; and C_S and C_{SC} are the heat capacities of the sample and the cell-sensor set. No equation for the power balance of the heat sink has been taken into account, since its heat capacity is so large that its temperature does not vary appreciably when involved in heat exchange processes.

The thermal relaxation times of the isolated elements, sample and cell-sensor set, are given by:

$$\tau_S = \frac{C_S}{\alpha_S} \qquad \tau_{SC} = \frac{C_{SC}}{\alpha_{SC}} \tag{3}$$

In these definitions no interaction between the elements has been considered.

Making the following transformation:

$$\Delta T_S(t) = T_S(t) - T_0$$

$$\Delta T_{SC}(t) = T_{SC}(t) - T_0 \tag{4}$$

the solution of the problem in the Laplace's transformed domain, with null initial conditions, is:

$$\Delta T_S(s) = \frac{\frac{1}{\alpha_S}\left(1 + \frac{\alpha_S}{\alpha_{SC}} + \frac{C_{SC}}{\alpha_{SC}}s\right)}{1 + \left(\frac{C_{SC}}{\alpha_{SC}} + \frac{C_S}{\alpha_S} + \frac{C_S}{\alpha_{SC}}\right)s + \frac{C_S C_{SC}}{\alpha_S \alpha_{SC}}s^2} W(s)$$

$$\Delta T_{SC}(s) = \frac{\frac{1}{\alpha_{SC}}}{1 + \left(\frac{C_{SC}}{\alpha_{SC}} + \frac{C_S}{\alpha_S} + \frac{C_S}{\alpha_{SC}}\right)s + \frac{C_S C_{SC}}{\alpha_S \alpha_{SC}}s^2} W(s) = g_{2P}(s)W(s) \tag{5}$$

where $\Delta T_{SC}(s)$ is the output signal of the two-element subsystem and, consequently, $g_{2P}(s)$ the transfer function.

Let us assume now that the thermal effect is produced directly on the cell-sensor set through an electrical calibration, $W(t)=W_E(t)$. The differential equation set corresponding to the thermal power balance, similar to the previous one (Eq. (2)), has the solution:

$$\Delta T_S(s) = \frac{\frac{1}{\alpha_{SC}}}{1 + \left(\frac{C_{SC}}{\alpha_{SC}} + \frac{C_S}{\alpha_S} + \frac{C_S}{\alpha_{SC}}\right)s + \frac{C_S C_{SC}}{\alpha_S \alpha_{SC}}s^2} W(s)$$

$$\Delta T_{SC}(s) = \frac{\frac{1}{\alpha_{SC}}\left(1 + \frac{C_S}{\alpha_S}s\right)}{1 + \left(\frac{C_{SC}}{\alpha_{SC}} + \frac{C_S}{\alpha_S} + \frac{C_S}{\alpha_{SC}}\right)s + \frac{C_S C_{SC}}{\alpha_S \alpha_{SC}}s^2} W(s) = g_{2P,\,0}(s)W(s) \tag{6}$$

It is observed that the new transfer function $g_{2P,0}(s)$ has two poles and one zero, whereas in the first case $g_{2P}(s)$ has only two poles and without zeros. This simple difference yields important consequences that will be shown later. A very significant fact is that the two poles are identical in the two different situations, since the characteristic equation (transfer function denominator) is the same.

Because sample and cell-sensor set are two interacting elements, the time constants of the system are not the same as the time constants of the each isolated element (Eq. (3)). They are given by:

$$\tau_1 = \frac{1}{p_1} \qquad \tau_2 = \frac{1}{p_2} \tag{7}$$

where p_1 and p_2 are the poles, real and dissimilar, of the transfer function, i.e. the roots of the characteristic equation:

$$s^2 + \left(\frac{\alpha_{SC}}{C_{SC}} + \frac{\alpha_S}{C_{SC}} + \frac{\alpha_S}{C_S} \right) s + \frac{\alpha_S \alpha_{SC}}{C_S C_{SC}} = (s + p_1)(s + p_2) = 0 \tag{8}$$

and the following relationship is fulfilled:

$$\tau_1 > \tau_S, \tau_{SC} > \tau_2 > 0 \tag{9}$$

The measured signal is a voltage (Fig. 2) because the flux sensors, semiconductor thermopiles, transform the temperature difference $\Delta T_{SC}(s)$ into a voltage $\Delta V_{SC}(s)$ (Seebeck effect):

$$\Delta V_{SC}(s) = \varepsilon_{SC} \Delta T_{SC}(s) \tag{10}$$

where ε_{SC} is the Seebeck coefficient of the sensor. In this way, the voltage produced by the sensors is:

$$\Delta V_{SC}(s) = \varepsilon_{SC} g(s) W(s) \tag{11}$$

where $W(s)$ represents $W_S(s)$ or $W_E(s)$, and $g(s)$ correspond to $g_{2P}(s)$ or $g_{2P,0}(s)$, according to the circumstances.

Since the microcalorimeter design is based on the twin principle, the treatment for the reference cell (RC) is completely analogous to the previous one and the thermal parameters are similar. If the thermopile sets of each cell are connected in opposition, the contributions to the total voltage generated by the sensors, $\Delta V_{SC}(s)$ and $\Delta V_{RC}(s)$, due to accidental effects are cancelled:

$$\Delta V(s) = \Delta V_{SC}(s) - \Delta V_{RC}(s) = \varepsilon (T_{SC}(s) - T_{RC}(s)) \tag{12}$$

where it has been assumed that: $\varepsilon_{SC} = \varepsilon_{RC} = \varepsilon$.

This voltage $\Delta V(s)$ is multiplied by an amplifier gain factor, A, obtaining the final output signal $\Delta V_{OUT}(s)$:

$$\Delta V_{OUT}(s) = A \Delta V(s) = A \varepsilon (T_{SC}(s) - T_{RC}(s)) \tag{13}$$

and for the two possible heat sources considered earlier:

$$\Delta V_{OUT}(s) = A \varepsilon g(s) W(s) = G(s) W(s) \tag{14}$$

where the factor $G(s)$ that multiplies to $W(s)$ represents the corresponding open-loop transfer function of the system, $G_{2P}(s)$ and $G_{2P,0}(s)$, in each case.

It is observed that time fluctuations of the heat sink temperature, T_0, do not affect the signal, since its effect is cancelled out: the measurement only depends on the temperature difference between both cells, caused mainly by the chemical reaction or the electrical calibration.

Microcalorimeter transfer function for a closed-loop control

In this configuration the microcalorimetric system is controlled through a compensation system with an active digital proportional control located in the feedback trajectory [11, 17, 18]. The compensation thermal power, $W_K(s)$, generated by the feedback transducer (compensation thermopiles), is given by:

$$W_K(s) = \frac{\pi}{R}\Delta V_C(s) + \frac{1}{R}\Delta V_C^2(s) \tag{15}$$

where $\Delta V_C(s)$ is the compensation voltage (feedback signal) and π and R are the Peltier coefficient and the electrical resistance of the transducer. The first term in the right hand side of this equation is the Peltier power and the second one is the Joule power. Taking 120 mV for the single junction Peltier coefficient [19], it can be established that the Joule power is negligible. It is always far less than 0.005 per cent of the total heat power generated, since $\Delta V_C(t)$ never exceeds 0.5 mV. Moreover, the compensation is made bilaterally and so the Joule effect is produced simultaneously in both cells and approximately cancelled. Therefore, if the compensator device consists of a pure proportional controller, the expression adopted for the compensation thermal power is:

$$W_K(s) = \frac{\pi}{R}\Delta V_C(s) = \frac{\pi}{R}K_p\Delta V_{OUT}(s) = G_{FB}(s)\Delta V_{OUT}(s) \tag{16}$$

where K_P is the proportionality constant of the feedback control. The factor multiplying to $\Delta V_{OUT}(s)$ is the feedback transfer function, $G_{FB}(s)$.

Taking into account that the compensation signal actuates on the cell-sensor set, it would be logical to consider for this thermal effect the transfer function with two poles and one zero. On the other hand, the sign of the transducer action in the reference cell is the opposite to that of the corresponding to the sample cell, thus implementing a symmetrical feedback system.

In order to obtain the closed-loop (global) system transfer function for a sample generated thermal effect, $G_S(s)$, the compensation power must be included in the global power balance:

$$\Delta V_{OUT}(s) = G_{2P}(s)\ W(s) - 2G_{2P,0}(s)W_K(s) \tag{17}$$

Substituting W_K by the Eq. (16) and reordering:

$$\Delta V_{OUT}(s) = \frac{G_{2P}(s)}{1 + 2G_{2P,0}(s)G_{FB}(s)} W(s) = G_S(s)W(s) \tag{18}$$

Similarly, we obtain the global transfer function for an electrical calibration, $G_E(s)$:

$$\Delta V_{OUT}(s) = \frac{G_{2P,0}(s)}{1 + 2G_{2P,0}(s)G_{FB}(s)} W(s) = G_E(s)W(s) \tag{19}$$

As a final step, both expressions (Eqs (18) and (19)) can be rewritten as:

$$\begin{aligned} G_S(s) &= A\frac{\varepsilon}{\alpha_{SC}}\frac{p_1p_2}{(s+p_1)(s+p_2)+bK_P(s+z_1)} = A\frac{\varepsilon}{\alpha_{SC}}\frac{p_1p_2}{(s+p_-)(s+p_+)} \\ G_E(s) &= A\frac{\varepsilon}{C_{SC}}\frac{(s+z_1)}{(s+p_1)(s+p_2)+bK_P(s+z_1)} = A\frac{\varepsilon}{C_{SC}}\frac{(s+z_1)}{(s+p_-)(s+p_+)} \end{aligned} \tag{20}$$

where p_- and p_+ are the poles of the system with feedback, b is a constant that contains some intrinsic parameters of the microcalorimeter and z_1 is the real zero of the transfer function, and they are given by:

$$b = 2A\frac{\varepsilon}{C_{SC}}\frac{\pi}{R} \qquad z_1 = \frac{\alpha_S}{C_S} \tag{21}$$

Despite that the transfer functions $G_S(s)$ and $G_E(s)$ differ in the presence of the zero z_1, the characteristic equation of both functions is identical:

$$(s+p_1)(s+p_2)+bK_P(s+z_1)=(s+p_-)(s+p_+)=0 \tag{22}$$

and the value of its roots, p_- and p_+ , depend on the feedback by means of the parameter K_P:

$$p_\pm = \frac{(p_1 + p_2 + bK_P) \pm \sqrt{(p_1 + p_2 + bK_P)^2 - 4(p_1p_2 + bK_Pz_1)}}{2} \tag{23}$$

The expression under the root of Eq. (23), i.e. the discriminant of the quadratic equation, Δ, can be rewritten as follows:

$$\Delta=(p_1-p_2+bK_P)^2+4bK_P(p_2-z_1)=(p_1-p_2-bK_P)^2+4bK_P(p_1-z_1) \tag{24}$$

Regarding that $p_1<z_1<p_2$ (Eq. (9)), it can be proved that the discriminant is positive for any value of K_P, positive, negative or null, and, therefore, the $p_\pm$ poles are real ones for any K_P value. The time constants of the microcalorimetric system under close-loop feedback control are now:

$$\tau_\pm = \frac{1}{p_\pm} \qquad \tau^* = \frac{1}{z_1} = \tau_S \tag{25}$$

Therefore, the time constant associated with the zero is equal to the thermal relaxation time of the sample considered as an isolated element, τ_S.

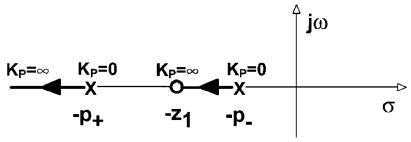

Fig. 3 Root locus diagram for Eq. (22) in the *s* plane. Pole ($p_{\pm}$) and zero (z_1) location represented by (X) and (O). It must be remembered that: σ=Re(*s*) and ω=Im(*s*)

Applying the root locus analysis [15, 16] to the characteristic equation (Eq. (22)) one can predict the influence of K_P on the behaviour of the microcalorimetric system for any parameter value from zero to infinity. In Fig. 3 the root locus in the *s* plane for $K_P \geq 0$ is shown. The pole and zero locations are represented by the symbols X and O, respectively. Bearing in mind the relationship $p_1 < z_1 < p_2$ (Eq. (9)) again, it is easy to see that:

$$p_{\pm} \in \mathrm{R}$$

$$0 < p_1 \leq p_- < z_1 < p_2 \leq p_+ \Rightarrow \tau_1 \geq \tau_- > \tau^* > \tau_2 \geq \tau_+ > 0$$

$$K_p = 0 \Rightarrow \begin{cases} p_- = p_1 \\ p_+ = p_2 \end{cases} \Rightarrow \begin{cases} \tau_- = \tau_1 \\ \tau_+ = \tau_2 \end{cases} \tag{26}$$

$$K_p \to +\infty \Rightarrow \begin{cases} p_- \to z_1 \\ p_+ \to \infty \end{cases} \Rightarrow \begin{cases} \tau_- \to \tau^* \\ \tau_+ \to 0 \end{cases}$$

The time constants, τ_- and τ_+, are decreasing functions of K_P, the decrease being due to the compensation. For a high enough value of K_P the pole p_+ is negligible and only it is necessary consider the pole p_-. In other words, the system would only have one time constant nearly equal to τ_S. In this way, with a highly efficient feedback, it would be possible to remove the thermal inertia of the cell-sensor element. Moreover, the system is always stable and does not become oscillatory for $K_P \geq 0$, since the poles are always real and negative.

If the existence of the zero z_1 is not taken into account and the root locus analysis is applied, it can be proved that the time constant τ_- is decreasing, but τ_+ is an increasing function of K_P. Also, for small K_P values the poles are real and negative, but from a particular K_P value the poles become complex conjugated with negative real part. This fact means that the system is still stable but with an oscillatory behaviour. This demonstrates that a compensation signal acting on the cell-sensor set and not on the sample directly is a recommended design strategy, instead of a design limitation.

If the Routh and Hurwitz stability criteria [15, 16] are applied, the following stability conditions appear:

$$K_P > -\frac{p_1 + p_2}{b} = -\frac{1}{b}\left(\frac{\alpha_{SC}}{C_{SC}} + \frac{\alpha_S}{C_{SC}} + \frac{\alpha_S}{C_S}\right)$$
$$K_P > -\frac{p_1 p_2}{b z_1} = -\frac{1}{b}\frac{\alpha_{SC}}{C_{SC}} \quad (27)$$

being the second inequality the determining condition, since it is more restrictive than the first one. Again, it is observed that the system is stable for $K_P \geq 0$. The same instability limit ($K_P = -p_1 p_2 / b z_1$) would have been obtained from the complementary root locus ($K_P \leq 0$).

Finally, we write the global (closed-loop) transfer function depending on the time constants and the steady state gain, G_0:

$$G_S = G_0 \frac{1}{(1 + \tau_- s)(1 + \tau_+ s)}$$
$$G_E = G_0 \frac{(1 + \tau^* s)}{(1 + \tau_- s)(1 + \tau_+ s)} \quad (28)$$

being:

$$G_0 = A \frac{\varepsilon}{\alpha_{SC}} \frac{1}{1 + a K_P}$$

and a is the dimensionless constant of the microcalorimetric system:

$$a = 2A \frac{\varepsilon}{\alpha_{SC}} \frac{\pi}{R} = b \frac{C_{SC}}{\alpha_{SC}} \quad (29)$$

Experimental transfer function determination

Once the physical model of the real system is defined, the transfer function can be determined from experimental observations. This is the so-called system identification problem, a common task in System Theory: from a known input, $x(t)$ or $X(s)$, and output, $y(t)$ or $Y(s)$, of the system one can obtain the transfer function, $G(s)$ or $g(t)$. The function $g(t)$ is called the unitary impulse response or the Green function. For a linear system the following relationships hold:

$$y(t) = \int_0^t g(t - t')x(t')\mathrm{d}t'$$
$$Y(s) = G(s)X(s) \quad (30)$$

in the time domain and in the Laplace's transformed domain, respectively.

On the other hand, if we want to identify $G(s)$ from $Y(s)$ and $X(s)$, these must be well defined and exactly known. Because it is difficult to specify how exactly is the mixing process when a chemical reaction is taking place in the calorimetric cell, the associated thermal effect is not well known. It is only possible to have an accurately defined input, X(s) or $x(t)$, if an electrical calibration is done.

As it has been proved that the transfer function poles are the same under identical experimental conditions irrespective of the thermal effect source (electrical calibration or chemical reaction), one can determine the transfer function parameters by means of an electrical calibration. For this purpose an electrically produced thermal effect corresponding to a finite width pulse has been used:

$$W(t) = W_0(\chi(t) - \chi(t-\Delta))$$
$$W(s) = W_0 \frac{1 - \exp(-s\Delta)}{s} \tag{31}$$

where W_0 is the constant Joule power developed during Δ seconds and $\chi(t)$ is the unitary step function ($\chi(t)$=0 for $t \leq 0$ and $\chi(t)$=1 for $t>0$). As the null width pulse (impulse), although formally easier to use, does not correspond with any physical event, only finite width pulses have been used as standard input function [2, 3].

The procedure is as follows [2]:

1. Analytical derivation of the microcalorimetric response to a finite width pulse:

$$\Delta V_{OUT}(t) = L^{-1}[G(s)W(s)], \quad \text{when} \quad W(s) = W_0 \frac{1 - \exp(-s\Delta)}{s} \tag{32}$$

Once the multiplication in the Laplace's transformed domain and the inverse Laplace transformation are made, we obtain the explicit expression of Eq. (32):

$$\Delta V_{OUT}(t) = A \frac{\varepsilon}{\alpha_{SC}} \frac{1}{1 + aK_P} W_0 \left(\left(1 - \beta \exp\left(-\frac{t}{\tau_-} \right) + \gamma \exp\left(-\frac{t}{\tau_+} \right) \right) - \right.$$
$$\left. - \left(1 - \beta \exp\left(-\frac{t-\Delta}{\tau_-} \right) + \gamma \exp\left(-\frac{t-\Delta}{\tau_+} \right) \right) \chi(t-\Delta) \right) \tag{33}$$

where the parameters β and γ are given by:

$$\beta = \frac{\tau_-}{\tau_- - \tau_+} \quad \gamma = \frac{\tau_+}{\tau_- - \tau_+}, \quad \text{when} \quad W(t) = W_S(t)$$
$$\beta = \frac{\tau_- - \tau^*}{\tau_- - \tau_+} \quad \gamma = \frac{\tau_+ - \tau^*}{\tau_- - \tau_+}, \quad \text{when} \quad W(t) = W_E(t) \tag{34}$$

2. Experimental recording of such response.

3. Fitting of experimental data to Eq. (33) by means of non-linear regression, in order to estimate the time constants, $\tau_{\pm}$ and τ^*.

Fitting is performed in the time domain to avoid the data processing problems that arise when sampled signals are used in frequency domain (Laplace or Fourier) [20].

To complete the transfer function evaluation, the steady state gain, G_0, must be experimentally determined. This calibration can be accomplished electrically by:

1. Pulses of finite width Δ and power W_0. The areas under the registered peaks of the signal $\Delta V_{OUT}(t)$ (Eq. (33)) are proportional to the corresponding heats Q, being G_0 the proportionality constant:

$$Area = \int_0^\infty \Delta V_{OUT}(t)\mathrm{d}t = G_0 W_0 \Delta = G_0 Q \tag{35}$$

2. Step inputs of constant power W_0. The steady state values of the registered signal $\Delta V_{OUT}(t)$ (Eq. (33)) are proportional to the corresponding delivered power W_0, being G_0 the proportionality constant:

$$\Delta V_{OUT}(+\infty) = \lim_{t\to+\infty}[\Delta V_{OUT}(t)] = G_0 W_0 \tag{36}$$

In this way, the instrumental calibration constant is defined as the inverse of the steady state gain, G_0:

$$K_{CAL} = \frac{1}{G_0} = \frac{1 + aK_P}{A\dfrac{\varepsilon}{\alpha_{SC}}} \tag{37}$$

Results and discussion

First of all, the two transfer function types are compared to evaluate the quality of the fit and the estimated values of the parameters (time constants). Figure 4 shows two fits to electrical calibration data from the Eq. (33), using the transfer function with only two poles (Panel A) and with two poles and one zero (Panel B). The time

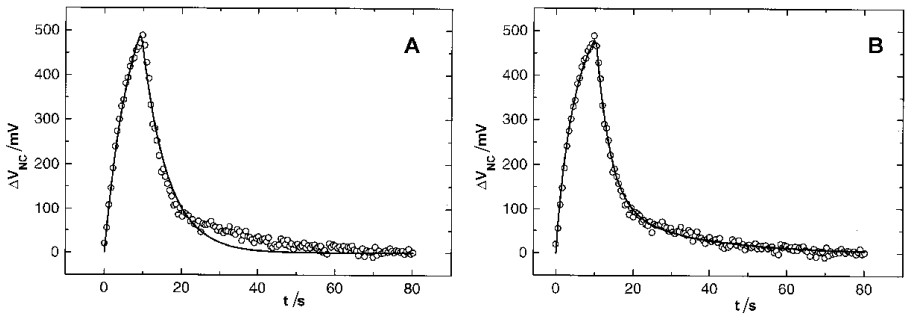

Fig. 4 Experimental response to a finite width power pulse with Δ=10*s*, W_0=167.5 μW and K_P=10×10^{-5} (open circles) and the fitted curve (solid line) for a transfer function with only two poles (panel A) and a transfer function with two poles and one zero (panel B)

Table 1 Time constants and χ^2 values obtained from the fits with the two types of transfer functions

	2 Poles	2 Poles + 1 Zero
$\tau_+(s)$	0.0±0.1	3.7±0.1
$\tau_-(s)$	6.7±0.2	26±1
$\tau^*(s)$	–	16±1
χ^2	365	69

constants obtained by non-linear regression and the corresponding χ^2 values are indicated in Table 1 for each transfer function. The fit with the first transfer function is worse than using the second one and, obviously, it gives incorrect time constants. In addition, this fit with the two poles transfer function must be rejected, since the critical value $\chi^2_{(145,0.05)}$ is 177 [21]. Consequently, taking into account the actual heat flux path in the heat power balance equations, i.e. the existence of the zero z_1 in the transfer function, it is possible to reproduce successfully the experimental curve. However, the transfer function with only two poles should be used for carrying out the dynamic correction of an output obtained from a chemical reaction. Therefore, depending on the heat source location, for determining the transfer function parameters and for performing a thermogram deconvolution the respective right transfer function must be used.

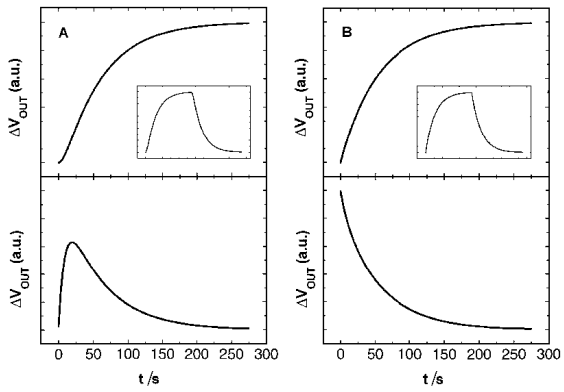

Fig. 5 Comparison between predicted responses for the two different transfer functions: Panel A: power step response (top) and power impulse response (bottom) for a transfer function with only two poles. The inset represents the finite width pulse response. Panel B: power step response (top) and power impulse response (bottom) for a transfer function with two poles and one zero. The inset represents the finite width pulse response

A detailed analysis of Eqs (33) and (34), taking into account the relationship between the time constants (Eq. (26)), allows us to predict the right response curves to standard power inputs frequently observed in calorimetry:

1. The step response to a sample generated thermal effect exhibits an inflexion point and a null initial slope, whereas the step response to a thermal effect generated on the cell-sensor set has not such singular point and a non null initial slope (Fig. 5).

2. The impulse response to a sample generated thermal effect consists of the difference of two decreasing exponential time functions, whereas the impulse response to a thermal effect generated on the cell-sensor set consists of the sum of two decreasing exponential time functions (Fig. 5). In both cases the system is really a second-order one. However, the presence of the zero in the transfer function modifies significantly the microcalorimeter behaviour and, apparently, the system looks like a first-order one.

Table 2 Influence of K_P on the time constants

	$K_P=0$	$K_P=5\times10^{-5}$	$K_P=10\times10^{-5}$	$K_P=20\times10^{-5}$
$\tau_+(s)$	8.1±0.3	5.4±0.1	3.8±0.1	2.5±0.1
$\tau_-(s)$	120±1	32.7±0.6	26.4±0.5	22±1
$\tau^*(s)$	16.2±0.6	16.3±0.4	15.8±0.5	16±1

The model predicts too that the time constants must be decreasing for increasing K_P values. Table 2 shows the influence of K_P on the time constants and the decreasing trend can be clearly seen. Moreover, the time constant associated with the zero is practically constant, with an approximated value of 16 s. This can be considered as a test for the model, since this time constant is the thermal relaxation time of the sample, τ_S, and it must remain invariable, independent of K_P.

In same way, the steady state gain is reduced by feedback compensation and as a consequence the calibration constant, as earlier defined (Eq. (37)), must increase. Therefore, the following model prediction has been checked: the calibration constant must exhibit an increasing linear behaviour with regard to K_P. Calibration ex-

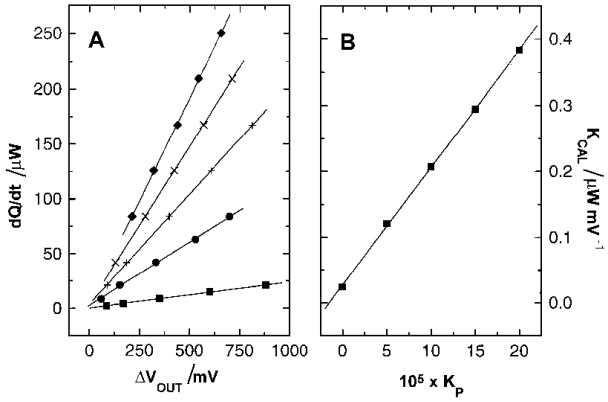

Fig. 6 Influence of K_P on the calibration constant K_{CAL}. Panel A: Heat power *vs.* steady state value $\Delta V_{OUT}(+\infty)$ for different K_P values. The calibration constants are obtained from the slope of the linear regressions. (■) $K_P=0$, (•)$K_P=5\times10^{-5}$, (+)$K_P=10\times10^{-5}$, (X)$K_P=15\times10^{-5}$, (♦)$K_P=20\times10^{-5}$. Panel B: Dependence of calibration constant on K_P

periments were carried out for different K_P values. Each calibration experiment consists of the application of successive step power inputs at fixed K_P value and the recording of the corresponding steady state values of the signal $\Delta V_{OUT}(+\infty)$. Figure 6 illustrates a set of linear fits to achieve the calibration constants for different K_P values (Panel A) and the dependency of the calibration constant on such K_P values (Panel B). The predicted linear behaviour is confirmed completely. The corresponding values of the calibration constant are shown in Table 3. According to Eq. (37), one can evaluate some instrumental parameters from the linear regression parameters. For example, values of 120±3 mV and 400±10 μV K^{-1} at 298 K are obtained for the single junction Peltier and Seebeck coefficient (two Bi_2Te_3 compensation thermopiles with an electrical resistance of 8.9±0.1 Ω and 66 semiconductor junctions each have been used). In the literature, values of 120 mV and 400 μV K^{-1} at 293 K for the thermoelectric coefficients of such semiconductor material [19] have been reported. This agreement supports the idea of that there is no appreciable heat leakage in the microcalorimeter. In addition, the calibration constant has been evaluated through the neutralisation reaction of NaOH with HCl [14] and the agreement is complete.

Table 3 Influence of K_P on the calibration constant

$10^5 \times K_P$	$K_{CAL}/\mu W\,mV^{-1}$
0	0.0240±0.0003
5	0.121±0.002
10	0.207±0.002
15	0.295±0.002
20	0.384±0.002

If we consider now the expression for the calibration constant (Eq. (37)) and the characteristic equation (Eq. (22)), the following result appears:

$$\tau_-\tau_+K_{CAL} = \frac{C_S C_{SC}}{\alpha_S}\frac{1}{A\varepsilon} \tag{38}$$

where τ_-, τ_+ and K_{CAL} are functions of K_P. However, the left hand of this equation must remain constant. Values of this term for different K_P values are indicated in Table 4, and the constancy of this quantity is observed. This is another test for the described model.

Table 4 Evaluation of the term $\tau_-\tau_+K_{CAL}$ for different K_P values

$10^5 \times K_P$	$\tau_-\tau_+K_{CAL}/s^2\mu W\,mV^{-1}$
0	23±1
5	21±1
10	21±1
20	21±2

Conclusions

A physical model of the microcalorimeter is presented. It is based on basic physical laws and it is not an empirical or phenomenological model. In view of the excellent fits obtained and the confirmed predictions, it seems that this is a realistic model for the real system. Likewise, it is a model valid for isothermal titration microcalorimeters in general, with and without compensation (K_P=0).

According to the model there are two different system transfer functions, depending on the heat source location. If the source is in the sample (chemical reaction) the transfer function contains two poles and if the source is on the cell-sensor set (electrical calibration) it has two poles and one zero. Choosing the right transfer function it is possible to reproduce the experimental data and to obtain a reliable microcalorimeter characterisation. Therefore, the adequate transfer function must be used for the system identification and for the thermogram deconvolution procedures, respectively.

A very simple and fast method for obtaining the transfer function of the microcalorimeter has been applied. No data processing in the frequency domain is required, since it only includes a non-linear fitting of the experimental raw data in the time domain.

The time constant associated with the zero has a very clear and simple physical meaning: this is the thermal relaxation time for the sample considered as an isolated element.

The feedback compensation modifies the system transfer function reducing the time constant associated with the poles (thermal inertia) and the thermogram peaks will be narrower and higher. We must keep in mind that the main time constant is a determining factor for the dynamic sensitivity [22], time resolution and overall time of an experiment run. All of them are important characteristics for microcalorimetric studies, specially when a slow kinetic process is involved in the chemical reaction. Moreover, it has been deduced that the compensation must be done on the cell wall; if it is done in the sample, the system becomes oscillatory for high K_P values.

It has been demonstrated that an accurate dynamic characterisation of the microcalorimeter can be achieved by means of a set of electrical calibrations, since the model establishes that the transfer function poles are the same for both chemical and electrical experiments. However, an accurate dynamic characterisation cannot be accomplished by means of chemical experiments because of the unknown time evolution of the associated thermal effect.

The model reported here can be generalised to a lumped parameter model with n elements holding all above mentioned results.

* * *

This research was supported by Projects PB96-1446 and MAT-98-0937-C02-01 from DGICYT and CICYT (Ministerio de Educación y Ciencia), Spain. One of us (A.V.C.) wishes to acknowledge the financial support of a Research Grant from the Junta de Andalucía, Spain.

References

1 C. Rey, Thermochim. Acta, 147 (1989) 145.
2 J. P. Dubes, R. Kechavarz and H. Tachoire, Thermochim. Acta, 79 (1984) 15.
3 K. R. Löblich, Thermochim. Acta, 231 (1994) 7.
4 K. H. Müller and Th. Plesser, Thermochim. Acta, 119 (1987) 189.
5 T. Yamane, S. Katayama and M. Todoki, Thermochim. Acta, 183 (1991) 329.
6 C. Rey, J. R. Rodríguez and V. Pérez-Villar, Thermochim. Acta, 61 (1983) 1.
7 J. Ortín, A. Ramos, V. Torra, J. Viñals and E. Margas, Thermochim. Acta, 76 (1984) 325.
8 O. López-Mayorga, P. L. Mateo and M. Cortijo, J. Phys. E: Sci. Instrum., 20 (1987) 265.
9 W. Zielenkiewicz, Thermochim. Acta, 204 (1992) 1.
10 E. Cesari, V. Torra, J. L. Macqueron, R. Prost, J. P. Dubes and H. Tachoire, Thermochim. Acta, 53 (1982) 1.
11 E. Freire, O. López-Mayorga and M. Straume, Anal. Chem., 62 (1990) 950A.
12 T. Wiseman, S. Williston, J. F. Brandts and L. Lin, Anal. Biochem., 179 (1989) 131.
13 M. El-Harrous, S. J. Gill and A. Parody-Morreale, Meas. Sci. Technol., 5 (1994) 1065.
14 J. Barthel, Thermometric Titrations, Ed. John Wiley & Sons, U.S.A., (1975).
15 B. C. Kuo, Sistemas de Control Automático, Ed. Prentice-Hall Hispanoamericana S.A., Mexico, 1996.
16 J. J. Distefano, A. R. Stubberud and I. J. Williams, Retroalimentación y Sistemas de Control, Ed. MacGraw-Hill, Colombia, 1992.
17 B. C. Kuo, Digital Control Systems, Ed. Saunders College Publishing, U.S.A., 1992.
18 J. R. Leigh, Applied Digital Control. Theory, Design and Implementation, Ed. Prentice-Hall, Great Britain, 1992.
19 C. J. Adkins, Termodinámica del Equilibrio, Ed. Reverté S.A., Spain, 1977.
20 A. V. Oppenheim and R. W. Schafer, Digital Signal Processing, Ed. Prentice-Hall, U.S.A., 1975.
21 J. H. Pollard, Numerical and Statistical Techniques, Ed. Cambridge University Press, Great Britain, 1977.
22 E. Margas and W. Zielenkiewicz, Thermochim. Acta, 215 (1993) 9.